Materials Science and Engineering B 172 (2010) 127–131

Contents lists available at ScienceDirect

Materials Science and Engineering B

journal homepage: www.elsevier.com/locate/mseb

Influence of heating on electric and magnetic properties of $Fe_{75}Ni_2B_{13}Si_8C_2$ amorphous alloy

D.M. Minić [a,*], A. Maričić [b]

[a] Military Technical Institute, Belgrade, Serbia
[b] Technical Faculty Čačak, University in Kragujevac, Serbia

ARTICLE INFO

Article history:
Received 25 January 2010
Received in revised form 20 April 2010
Accepted 28 April 2010

Keywords:
Amorphous materials
Electrical measurements
Magnetic Measurements

ABSTRACT

The influence of heating on the electrical and magnetic properties of $Fe_{75}Ni_2B_{13}Si_8C_2$ amorphous alloy is studied under non-isothermal as well as under isothermal conditions. According to thermal analysis the amorphous alloy was stable up to a temperature of about 500 °C when the process of multi-step structural transformations begins. According to the X-ray diffraction analysis, the primary crystallization starts by forming iron–silicon (Fe_3Si, 70 wt%) as main phase and two minor phases, iron–boron (Fe_2B, 10 wt%) and iron–boron–silicon ($Fe_{15}B_2Si_3$, 20 wt%). With the increase of the temperature, the change of weight composition, as well as the ratio of present phases occurs, and at 650 °C it was confirmed the presence of only two stable phases, Fe_3Si (74 wt%) and Fe_2B (26 wt%). It was shown that the observed change of structure had significant influence on both the electric and magnetic properties of alloy. The electric resistivity in crystallized alloy is higher than the amorphous one, but the crystallized alloy possesses better magnetic susceptibility and retains the ferromagnetic properties in the whole investigated temperature range.

1. Introduction

Amorphous alloys, also known as "metallic glasses" are materials obtained by rapid quenching of melt at a cooling rate of about 10^5–10^6 K s^{-1} in conditions where the crystallization is suppressed [1]. These materials possess a disordered distribution of atoms in the cooled melt and an excellent combination of physical properties which are very important for their high technological applications [2]. The soft magnetic amorphous alloys are based on the ferromagnetic elements, Fe, Co and Ni, containing the glass forming elements such as Si, B, C and P [3]. The most stable amorphous alloys contain about 80 at% of transition metal (ferromagnetic elements) and 20 at% metalloid components (glass forming elements) [4]. Because of their excellent soft magnetic properties, such as high saturation magnetization, high permeability, low coercivity and loss, these materials have many different applications, such as power devices, information handling technology, magnetic sensors, antiheft security systems [5–7]. The amorphous alloys are metastable materials so the elevated temperature as well as the prolonged performance could induce the process of change in their microstructure [8]. The formed microstructure usually involves the nanocrystals about 10 nm in size, embedded in an amorphous matrix possessing soft magnetic properties superior to the amorphous and conventional crystalline magnetic alloys of the same composition [9,10]. However the crystallization of amorphous alloys can provoke the formation of crystalline phases that deteriorates their advanced properties making them useful only once. However, it is well known that the magnetic properties, as well as the electric properties, of these materials are structurally very sensitive and depend significantly on the manufacturing conditions of the alloys as well as their thermal history [8]. For technological applications, nanostructured soft magnetic alloys obtained by partial crystallization from amorphous precursors are very important [11,12]. Therefore knowing the thermal stability, pressure effects, surface effects, microstructure, kinetic crystallization as well as the effects of composition are of great interest for technological applications amorphous and nanostructured materials. The thermal stability and structural transformation of amorphous $Fe_{75}Ni_2B_{13}Si_8C_2$ alloy were studied previously [13]. It was found that the alloy were stable up to temperature of 450 °C when the crystallization began by forming the crystal Fe_3Si phase in an amorphous matrix. At higher temperatures the presence of the other two phases (Fe_2B and $Fe_{15}B_2Si_3$) were noticed. The crystallization process starts with the formation of nanosized crystallites whose further growth is temperature dependent.

In this paper we have studied in detail the influence of temperature (the temperature range 25–600 °C) on structure of amorphous $Fe_{75}Ni_2B_{13}Si_8C_2$ alloy in order to find the influence of the structural transformations on the electric and magnetic properties of alloy.

* Corresponding author. Tel.: +381 11 251 3091.
E-mail address: dminic2003@yahoo.com (D.M. Minić).

0921-5107/$ – see front matter © 2010 Elsevier B.V. All rights reserved.
doi:10.1016/j.mseb.2010.04.034

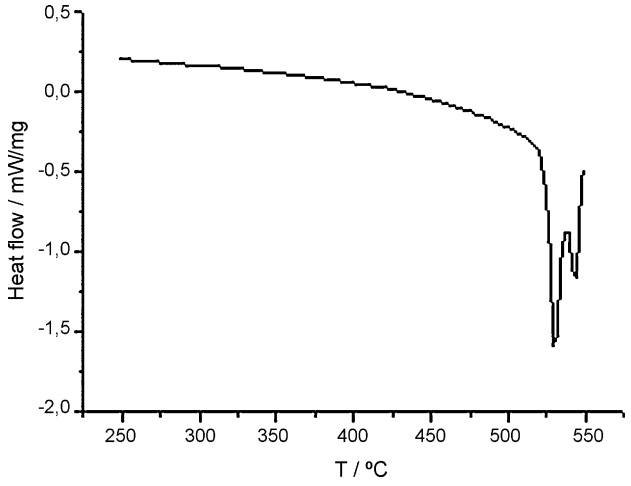

Fig. 1. DSC curve for $Fe_{75}Ni_2B_{13}Si_8C_2$; heating rate 5 °C min^{-1}.

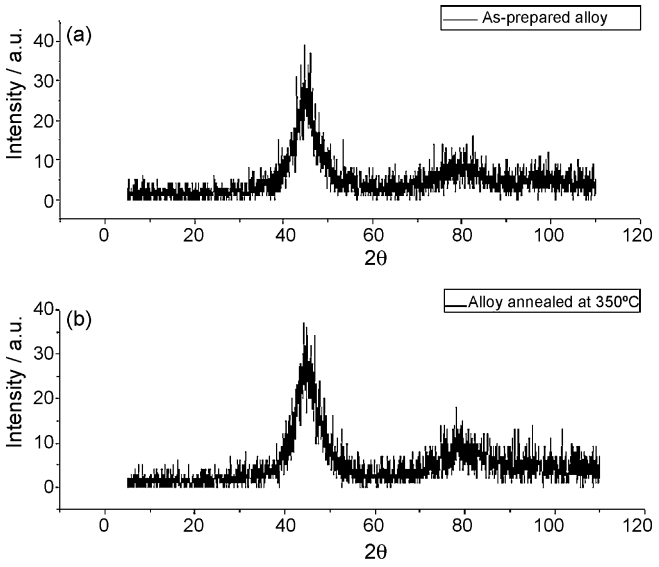

Fig. 2. XRD spectra of as-prepared alloy and sample of alloy annealed at 350 °C.

2. Experimental procedure

The ribbon-shaped samples of the $Fe_{75}Ni_2B_{13}Si_8C_2$ amorphous alloy were obtained using the standard procedure of rapid quenching of the melt on a rotating disc (melt-spinning). The resulting ribbon was 2 cm wide and 35 μm thick.

The crystallization process was investigated by the DSC technique in a nitrogen atmosphere using a SHIMADZU DSC-50 analyzer. In this case, samples weighing several milligrams were heated in the DSC cell from room temperature to 600 °C in a stream of nitrogen with a flow rate of 20 mL min^{-1} and a heating rate of 20 °C min^{-1}.

In order to investigate the structural transformations by the XRD technique, the samples of the amorphous alloy $Fe_{75}Ni_2B_{13}Si_8C_2$ were annealed at the different temperatures (25–850 °C) in a stream of nitrogen during 30 min. The X-ray powder diffraction patterns for the as-prepared alloy, as well as for the samples that were annealed at different temperatures, were recorded on a Philips PW-1710 automated diffractometer using a Cu tube operated at 40 kV and 30 mA. The instrument was equipped with a diffracted beam curved graphite monochromator and Xe-filled proportional counter. For the routine characterization, the diffraction data were collected in the range of 2θ Bragg angles (4–100° counting for 0.1 s). Silicon powder was used as an external standard for the calibration of the diffractometer. All XRD measurements were done with solid ribbon-shaped samples at ambient temperature. For a quantitative analysis and determination of crystallite size we used HighScore plus with Rietweld structural models based on the ICSD database.

The electrical resistance of the ribbon was measured by the four-point method within a temperature range of 20–600 °C in an argon atmosphere. Measurements of relative magnetic permeability were performed using a modified Maxwell method, based on the action of an inhomogeneous magnetic field on a magnetic sample. The magnetic force measurements were performed with a sensitivity of 10^{-6} N in an argon atmosphere.

3. Results and discussion

The thermal stability of this alloy was investigated by thermal analysis in the temperature interval of 20–550 °C at a heating rate of 5 °C min^{-1}. The obtained DSC curve, Fig. 1, involves only two poorly separated exo-peaks with maximum at 529.2 and 544.2 °C, respectively, indicating a stepwise process of a thermal stabilization of alloy.

The amorphous state of the as-prepared alloy was confirmed by the X-ray diffraction method. The diffraction pattern for the as-prepared alloy, as well as of the alloy isothermally heated at 350 °C, Fig. 2, involves only a spread halo in the 2θ range of 40–50° and does not involve appreciable diffraction peaks, indicating the absence of any long-range crystalline order. This behavior is characteristic for an amorphous structure which remained unchanged after annealing at 350 °C. The size of the coherently scattering regions, calculated from the half-width of the observed halo by Scherrer's formula, is about 0.86 nm, pointing out the presence of highly disordered Fe clusters in an amorphous matrix.

The samples of amorphous ribbon in the as-prepared state was repeatedly vacuum-annealed during 30 min at the temperatures before and after maxima at DSC curves (450, 510, 530, 550, 650, 750 and 8750 °C) in order to clarify the features of the thermal induced changes. The obtained diffractograms are presented in Fig. 3. These diffractograms show that the thermally induced structural changes started at 450 °C. For the qualitative determination of the phase composition of the crystallized alloy samples, the JCPDS-PDF database has been used. Besides the phase composition, the quantitative calculation of the contents of each individual phase was obtained using the Rietveld's refinement procedure [14]. This procedure is able to simulate the XRD pattern from given starting parameters. For this purpose the Rietveld's refinement program TOPAS V 3.0 (Bruker AXS GmbH, Germany) was used [15]. The quality of the refinement progress was controlled by monitoring the fit parameter R_{wp}, the goodness of fit (GOF), and the Durbin–Watson factor.

The diffraction pattern of the annealed alloy at 450 °C, Fig. 3, contains the same halo as the original sample as well as a sharp peak at $2\theta = 44.95°$ and a few small peaks indicating the presence of a crystal phase in amorphous matrix. An increase of the annealed temperature results in the appearance of new sharp peaks corresponding to the presence of the Fe_3Si (70 wt%) phase which is isotopic to gupeiite [JCPDS-PDF 03-065-0146]. At the same time, after annealing of alloy at higher temperatures (510 and 530 °C) besides the intense diffraction peaks of the Fe_3Si phase, the presence of the weak peaks corresponding to the Fe_2B phase (10 wt%) [JCPDS-PDF 03-065-2693] and $Fe_{15}B_2Si_3$ phase (20 wt%) [JCPDS-PDF 00-047-1629] became noticed.

At the higher temperature of annealing (650 and 750 °C) the peaks of the $Fe_{15}B_2Si_3$ phase completely disappear and the pres-

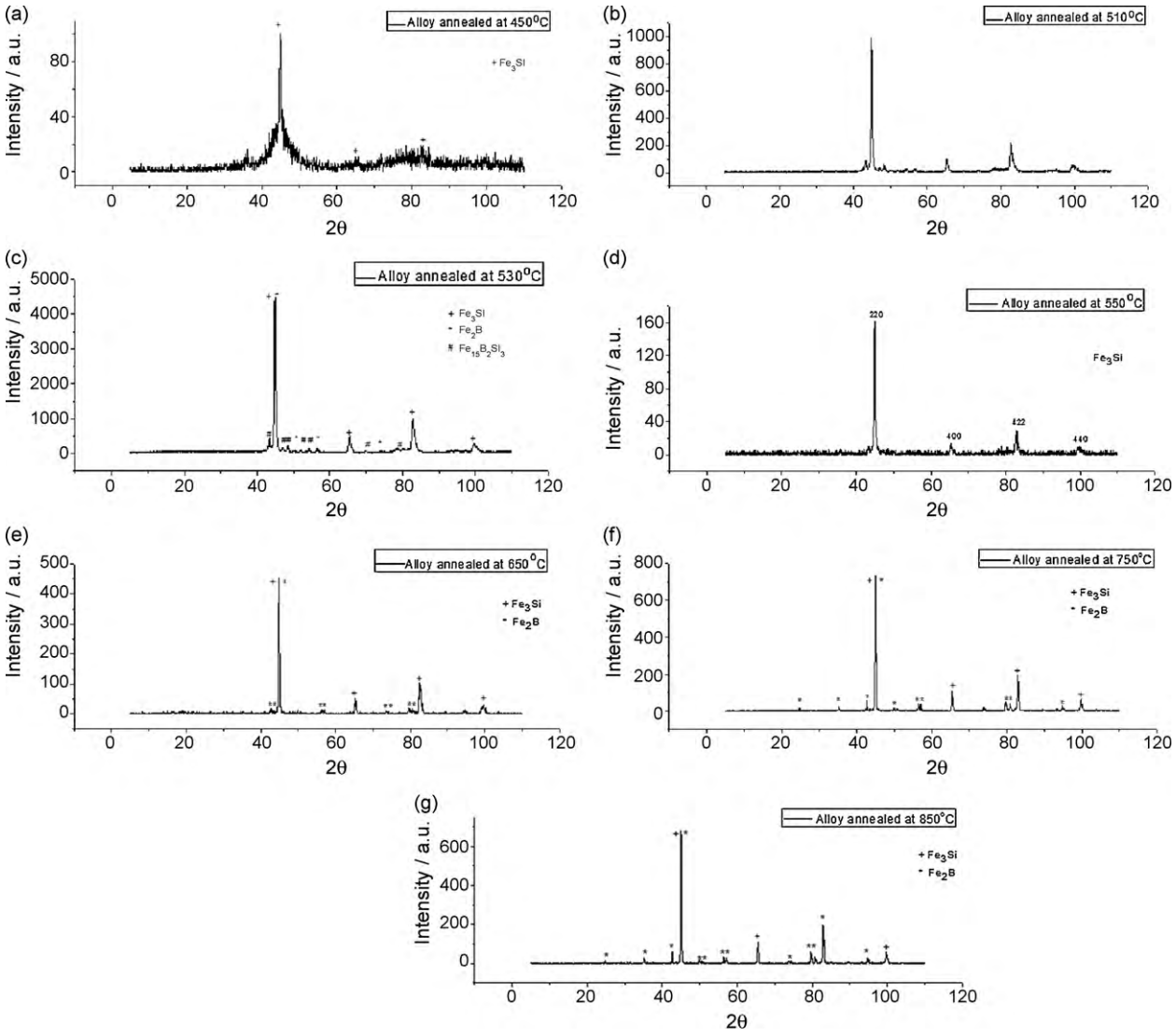

Fig. 3. XRD spectra of samples of alloy annealed at different temperatures.

ence of only two phases (Fe_3Si, 74 wt% and Fe_2B, 26 wt%) was noticed.

Furthermore, the increase of the heating temperature, as well as the extension of heating time, leads to an increase of the intensities of all the present peaks pointing to the better crystallization of all the present phases, as well as the growth of formed crystals.

It shows that the crystallization process starts with nanosized crystallites, and their growth is further temperature dependent, leading to the formation of phases Fe_3Si and Fe_2B in almost equal quantity [13].

The relative magnetic susceptibility of the as-prepared $Fe_{75}Ni_2B_{13}Si_8C_2$ amorphous alloy was measured non-isothermally in different temperature ranges, before as well as after the crystallization of alloy. The magnetic moment is very sensitive on changes in atomic magnetic characteristics because of phase or structure transitions. The obtained temperature dependences of the relative magnetic susceptibility for five sequential cycles of heating alloy to different temperatures before as well after the crystallization of alloy are presented in Fig. 4. The appearance of the thermomagnetic curves indicates all kinds of changes in material magnetic moment induced by heating the alloy. The most pronounced change on shown thermomagnetic curve, Fig. 4a, represents the Curie point (T_c = 410 °C), where the magnetization of appropriate phase falls almost to zero, because the magnetic interaction cannot resist the thermal motion any more. The annealing at the temperatures in the range 200–400 °C is sometimes called a "stress-relieving transformation" and usually influences the physical properties of the amorphous material. In this process, internal strains and the free volume are reduced in the starting material. These changes are accompanied by subtle inter-atomic movements, causing the changes in the electron structure. This leads to an increase in the number of electrons with unpaired spin in the direction of the outer magnetic field; this also leads to a decrease in the number of electrons spinning in the reverse direction and causes an increase in the magnetic susceptibility upon cooling. At the same time, strains and a decrease in the free volume during structural relaxation enable greater mobility of the walls of the magnetic domains, and this behavior further contributes to the increase in the magnetic susceptibility.

During further heating, it is noticed the decrease in the magnetic susceptibility in the temperature region from 350 to 410 °C as a result of getting closer to the Curie temperature of the amorphous alloy.

During further heating, above 410 °C, the alloy loses its ferromagnetic properties. After the first heating up to 450 °C, Fig. 4a, the magnetic susceptibility of relaxed alloy increases by 18% as com-

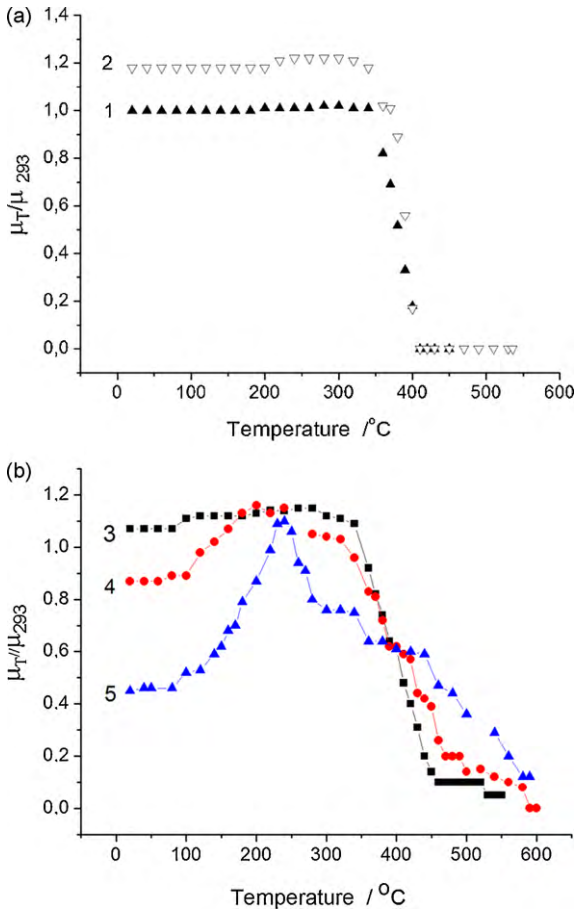

Fig. 4. (a) Temperature dependence of the relative magnetic susceptibility of alloy: first heating up to 450 °C and second heating up to 536 °C. (b) Temperature dependence of the relative magnetic susceptibility of alloy: third heating up to 550 °C; fourth heating up to 600 °C; and fifth heating up to 610 °C.

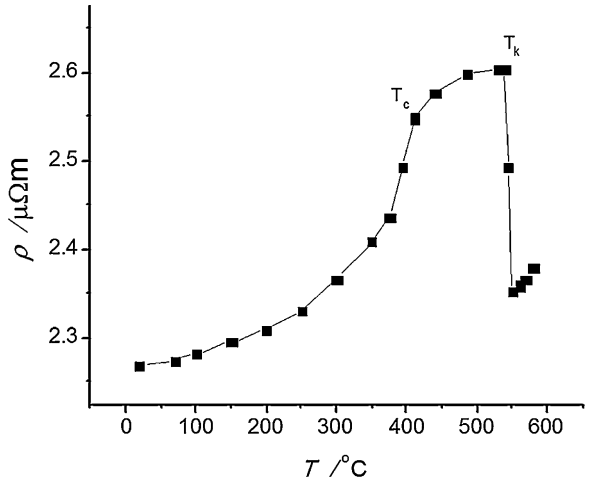

Fig. 5. Temperature dependence of the electrical resistivity of as-prepared alloy.

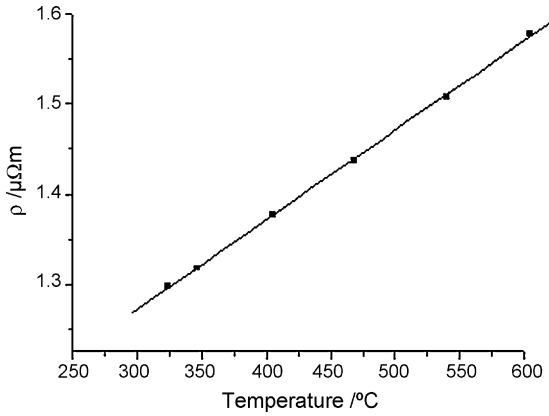

Fig. 6. Temperature dependence of the electric resistivity of the crystallized alloy.

pared to the value in its amorphous state. The partially crystallized alloy (after heating up to 536 °C) as well as crystallized alloy after heating above the crystallization temperature, Fig. 4a, maintain their ferromagnetic features in the whole temperature region. The observed change in the magnetic susceptibility is a consequence of further phase transformation of the crystallized alloy.

Generally speaking the electrical resistivity of the ordered (crystalline) alloy is lower than the disordered (amorphous) alloy of the same composition, Figs. 5 and 6. The temperature dependence of electrical resistivity clearly shows each structural stabilization step which causes the change in the ordering of the investigated material.

The temperature dependence of the electrical resistivity of the as-prepared alloy in the temperature range of 20–600 °C is shown in Fig. 5. The slow increase of electrical resistivity in the temperature range of 250–400 °C was caused by the structural relaxation processes occurring in alloy during heating. These processes further are followed by a sharp increase of electrical resistivity in the vicinity of Curie temperature (T_c = 410 °C). At this point the effect of scattering of conductive electrons on the magnons disappeared, and the amorphous alloy loses its ferromagnetic features. The beginning of crystallization at about 530 °C causes the sharp drop of electrical resistivity. During heating up to 600 °C, the alloy crystallizes, getting lower electrical resistivity. The temperature dependence of the electrical resistivity of the alloy in the second heating is shown in Fig. 6. The linear change of electrical resistivity with the rising temperature during the second heating of the alloy showed that the process of crystallization was completed during the first heating up to 600 °C. The crystallized alloy has significant lower electrical resistivity as could be expected for an ordered structure that the alloy possesses.

4. Conclusion

Thermal treatment of the $Fe_{75}Ni_2B_{13}Si_8C_2$ amorphous alloy by heating in the temperature range 20–750 °C, under non-isothermal as well as under isothermal conditions, provoked the series of structural transformations of alloy involving the stress-relieving transformation at the temperatures in the range 200–400 °C, the loss of ferromagnetic features at Curie temperature (410 °C), and finally the stepwise process of crystallization at the higher temperatures. According to the X-ray diffractograms, the primary crystallization starts at 450 °C by forming Fe_3Si as main phase what was followed by forming two less present phases: Fe_2B and $Fe_{15}B_2Si_3$. With the increase of the temperature, the weight composition, the ratio of all present phases as well as the size of formed crystallites are changed. Above 550 °C it was confirmed the presence of only two stable phases, Fe_3Si (74 wt%) with the crystallite size of 30 nm and Fe_2B (26 wt%) with the crystallite size of 6 nm. The increase of temperature provokes the further growth of formed crystallites. All observed that structural transformations provoke the change of the electric and magnetic properties of alloy. The electric resistivity of alloy increases with temperature up to the beginning of crystallization and then suddenly drops. The crystallized alloy possesses lower electrical resistivity than an amorphous one, but the crystallized alloy possesses better mag-

netic susceptibility and retains the ferromagnetic properties in the whole investigated temperature range.

Acknowledgement

The investigation was supported by the Ministry of Science and Environmental Protection of Serbia, under the Project 142011G. The authors are grateful to A. Gavrilovic and L. Rafailovic (ECHEM Kompetenzzentrum fur angewandte Electrochemie GmbH, A-2700 Weiner Neustadt, Austria) for X-ray and DSC data.

References

[1] J.S. Blazquez, M. Millan, C.F. Conde, V. Franco, A. Conde, S. Lorenzo-Perez, J. Non-Cryst. Solids 354 (2009) 5135.
[2] D.M. Minić, Sci. Sintering 38 (2006) 83.
[3] K. Biswas, S. Ram, I. Schultz, J. Eckert, J. Alloys Compd. 397 (2005) 104.
[4] S.D. Kaloshkin, I.A. Tomlin, Thermochim. Acta 280–281 (1996) 303.
[5] I.C. Rho, C.S. Yoon, C.K. Kim, T.Y. Byun, K.S. Hong, Mater. Sci. Eng. B 96 (2002) 48.
[6] T. Gloriant, S. Surinah, M.D. Baro, J. Non-Cryst. Solids 333 (2004) 48.
[7] M. Miglierini, J. Non-Cryst. Solids 354 (2009) 5093.
[8] M.G. Scott, in: F.E. Luborsky (Ed.), Amorphous Metallic Alloys, Butterworths, London, 1983, p. 144.
[9] H.F. Li, R.V. Ramanjujan, Mater. Sci. Eng. A 375 (2004) 1087.
[10] J. Bednarick, R. Nicula, M. Stir, E. Bukel, J. Magn. Magn. Mater. 316 (2007) e823.
[11] M.A. Willard, V.G. Harris, JOM 3 (2002) 44.
[12] M.E. McHenry, M.A. Willard, D.E. Laughlin, Prog. Mater. Sci. 44 (1999) 291.
[13] D.M. Minić, A. Gavrilović, P. Angerer, D.G. Minić, A. Maričić, J. Alloys Compd. 476 (2009) 705.
[14] H. Rietveld, J. Appl. Crystallogr. 2 (1969) 65.
[15] Bruker AXS, TOPAS V3: general profile and structure analysis software for powder diffraction data, Karlsruhe, 2005.